Electronic Supplementary Information

Experimental section

Materials: Nafion (5 wt%) solution, salicylic acid, ammonium heptamolybdate ($(NH_4)_6Mo_7O_{24}\cdot 4H_2O$), sodium citrate, sodium hypochlorite (NaClO), sodium nitroferricyanide ($C_5FeN_6Na_2O$), para-(dimethylamino) benzaldehyde, and aniline were purchased from Sigma-Aldrich Chemical Reagent Co., Ltd. Hydrochloric acid (HCl) and ethanol were purchased from Aladdin Ltd. (Shanghai, China). Nafion 115 membrane (DuPont) was purchased from HESEN Co., Ltd. (Shanghai, China). Ultrapure water used throughout all experiments was purified through a Millipore system.

Preparation of MoO_2/GCE: 2.48 g $(NH_4)_6Mo_7O_{24}\cdot 4H_2O$ and 3.20 g aniline were added to aqueous solution (40 mL) and the pH was adjusted to 4-5 with HCl (1 M) in drop-wise manner. After stirring for 6 h at 50 °C, the obtained product was washed with ethanol and dried at 65 °C. The MoO_2 was obtained. The MoO_2 ink was prepared by dispersing 5 mg of MoO_2 catalyst into 980 μL of water/ethanol (v/v = 1:1) solvent containing 20 μL of 5 wt% Nafion and sonicated for 1 h. Then 5 μL of the MoO_2 ink was loaded onto a well-polished GCE surface. The MoO_2/GCE was prepared well.

Preparation of Mo_2N /GCE: MoO_2 was calcined at 700 °C for 3 h in an ammonia gas flow. After cooled to room temperature, Mo_2N nanorod powder was obtained. To avoid the adsorbed NH_3 affecting result, Mo_2N powder was washed with HCl (0.1 M) for three times. Mo_2N ink was prepared by dispersing 5 mg of Mo_2N catalyst into 980 μL of water/ethanol (v/v = 1:1) solvent containing 20 μL of 5 wt% Nafion and sonicated for 1 h. Then 5 μL of the Mo_2N ink was loaded onto a well-polished GCE surface.

Characterizations: XRD patterns were obtained from a Shimazu XRD-6100 diffractometer with Cu Kα radiation (40 kV, 30 mA) of wavelength 0.154 nm (Japan). SEM images were collected from the tungsten lamp-equipped SU3500 scanning electron microscope at an accelerating voltage of 20 kV (HITACHI, Japan). TEM images were obtained from a Zeiss Libra 200FE transmission electron microscope

operated at 200 kV. XPS measurements were performed on an ESCALABMK II X-ray photoelectron spectrometer using Mg as the exciting source. The absorbance data of spectrophotometer were measured on SHIMADZU UV-1800 ultraviolet-visible (UV-Vis) spectrophotometer.

Electrochemical measurements: Before NRR tests, the Nafion 115 membrane was pre-treated by heating in 5% H_2O_2 solution and ultrapure water at 80 °C for 1 h, respectively. Electrochemical measurements were performed with a CHI 660E electrochemical analyzer (CHI Instruments, Inc., Shanghai) in a standard three-electrode system using Mo_2N/GCE as working electrode, Ag/AgCl as reference electrode, and graphite rod as counter electrode. All experiments were carried out at room temperature (25 °C). For N_2 reduction experiments, the HCl electrolyte (0.1 M) was bubbled with N_2 for 30 min before the measurement.

Nafion resistance analysis: To evaluate the resistance of Nafion membrane, two kinds of conditions were conducted: one compartment cell testing and two compartment cell testing. The resistance of Nafion membrane can be regarded as the resistance of solution, which is denoted as R_Ω.. From Fig. S1, the resistance of Nafion membrane is the difference of two values of R_Ω. That is 9.75 Ω at -0.3 V (the best NRR rate), and the current is 0.2 mA. The difference in potential loss is 9.75×0.2 = 2 mV. Thus, the resistance of Nafion membrane can be ignored. Meanwhile, the fitting values of one-compartment cell are R_{s1}=2.21 ohm, R_{ct1}=1.66 ohm, and C_{dl}=0.0639 F. The fitting values of two-compartment cell are R_{s2}=24.9 ohm, R_{ct2}=2.68 ohm, and C_{d2}=0.0428 F.

Determination of NH_3: The produced ammonia was estimated by indophenol blue method by ultraviolet spectroscopy. In detail, 2 mL of post-tested solution was got from the electrochemical reaction vessel. Then, 2 mL of 1 M NaOH solution (contains 5 wt% salicylic acid and 5 wt% sodium citrate) was followed by addition of 1 mL of 0.05 M NaClO and 0.2 mL of $C_5FeN_6Na_2O$ (1 wt%). After standing at 25 °C for 2 h, the UV-Vis absorption spectrum was measured. The concentration of indophenol blue was determined using the absorbance at awavelength of 655 nm. The concentration-absorbance curve was calibrated using standard ammonia chloride solution with a

serious of concentrations. The fitting curve ($Y=0.336X+0.018$, $R^2=0.999$) shows good linear relation of absorbance value with NH_4Cl concentration by three times independent calibrations.

Determination of N_2H_4: The N_2H_4 present in the electrolyte was determined by the method of Watt and Chrisp. The p-$C_9H_{11}NO$ (5.99 g), HCI (30 mL), and C_2H_5OH (300 mL) were mixed and used as a color reagent. In detail, 5 μL electrolyte was removed from the electrochemical reaction vessel, and added into 5 mL prepared color reagent and stirred 15 min at 25 °C. The obtained calibration curve of N_2H_4 is $Y=0.552X + 0.044$, $R^2=0.995$.

Calculations of NH_3 formation rate and FE: Ammonia formation was calculated using the following equation:

$$\text{Ammonia formation rate} = [NH_4^+]\times V/(m\times t)$$

FE was calculated according to following equation:

$$FE = 3\times F\times[NH_4^+]\times V/(17\times Q)$$

Where $[NH_4^+]$ is the measured NH_4^+ ion concentration; V is the volume of the cathodic reaction electrolyte; t is the potential applied time; m is the loaded quality of catalyst; F is the Faraday constant; and Q is the quantity of applied electricity.

Calculations of H_2 amount and FE: The FE was calculated by comparing the amount of measured H_2 generated by cathodal electrolysis with calculated H_2 (assuming 100% FE). GC analysis was carried out on GC–2014C (Shimadzu Co.) with thermal conductivity detector and nitrogen carrier gas. Pressure data during electrolysis were recorded using a CEM DT-8890 Differential Air Pressure Gauge Manometer Data Logger Meter Tester with a sampling interval of 1 point per second.

FE was calculated according to following equation:

$$FE = 2\times F\times n/Q$$

Where F is the Faraday constant; n is the actually produced H_2(mol), and Q is the quantity of applied electricity.

Computational Methods: DFT calculations were performed using the Vienna Ab initio Simulation Package (VASP).[1] The Perdew-Burke-Ernzerhof functional (PBE)[2] was employed with the projector augmented wave (PAW)[3] pseudo potentials. Energy

cutoff for the plane wave was 500 eV. The convergence threshold of structure relaxation was set to be 0.025 eV/Å. The Brillouin zone was sampled with 3×3×1 Monkhorst-Pack k-point mesh. Based on various facets, slab models were built with vacuum layer of 20 Å to avoid the interaction between the periodic images. Surface energies, E_{surf} , were computed from:

$$E_{surf}=(E_{slab}-N*E_{bulk})/A$$

Where E_{slab} is the energy of the slab model; E_{bulk} is the energy of the bulk unit cell; N is the number of unit in the slab and A is the surface area. From Table S3, $Mo_2N(100)$ and $MoO_2(100)$ are considered to be the most energetically favored surfaces. Free energy of each adsorbed species was from optimization and frequency calculations: G=E+ZPE-TS. E, ZPE and S denote total energy, zero-point energy and entropy, respectively. T equals to 298.15 K. Thermal corrections for gas molecules are from database.[4]

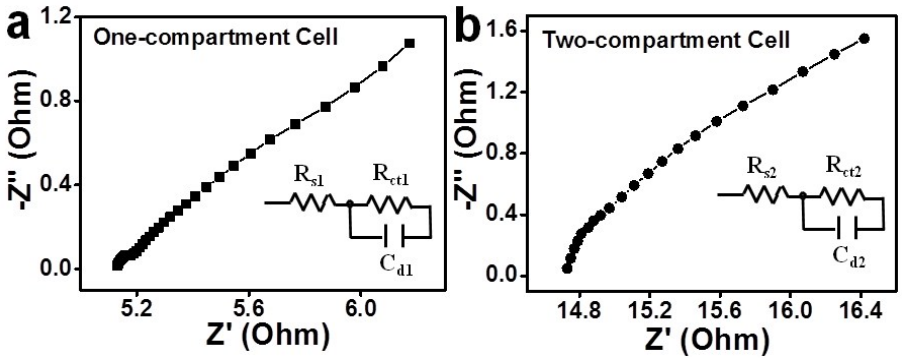

Fig. S1. EIS spectra of two kinds of testing conditions: (a) all the three electrodes are in one compartment cell; (b) the working electrode/reference electrode and the counter electrode are in two compartment cell separated by Nafion 115 membrane. (inset: an equivalent circuit model; R_s: series resistance; R_{ct}: charge transfer resistance; C_d: capacitance)

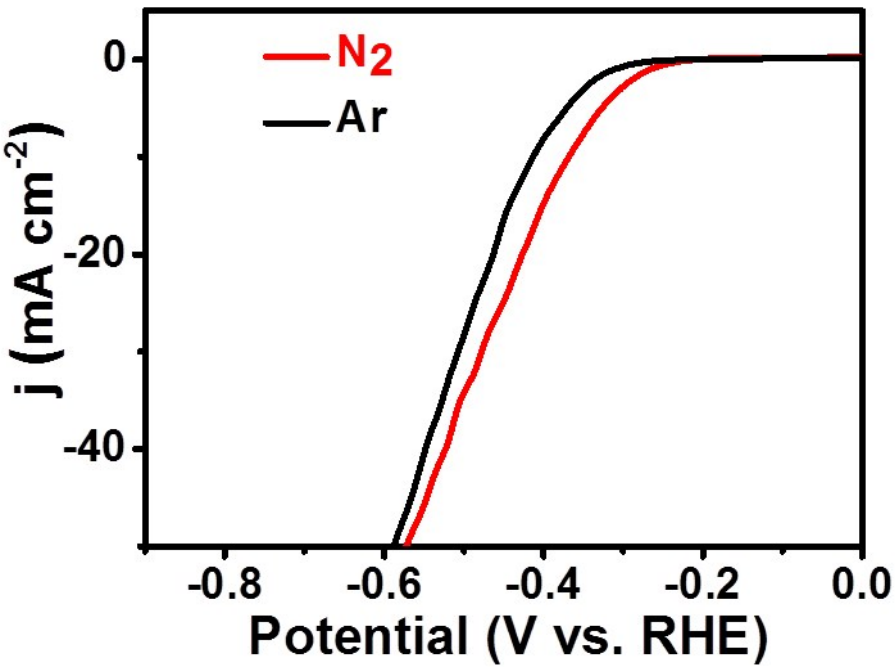

Fig. S2. LSV curves for electrocatalytic NRR of Mo_2N/GCE in N_2- (red line) and Ar-saturated (black line) electrolytes

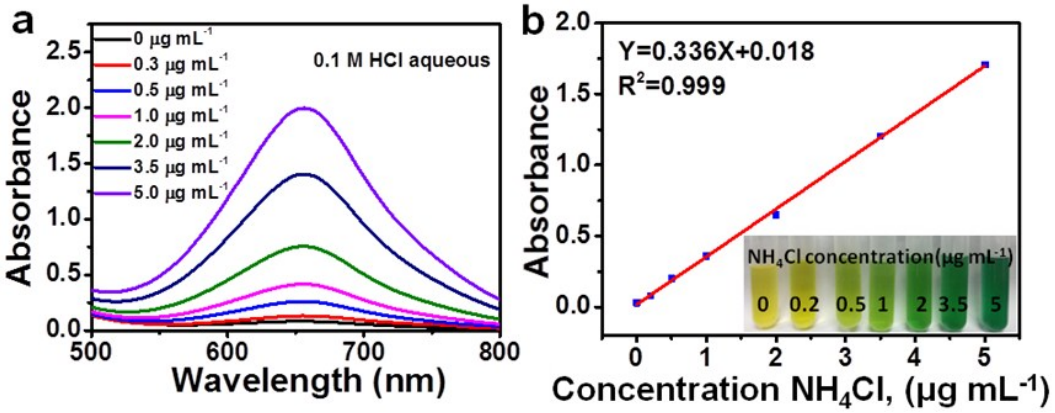

Fig. S3. (a) UV-Vis spectra of indophenol assays with NH_4^+ ions after incubated for 2 h at room temperature. (b) Calibration curve used for estimation of NH_4Cl.

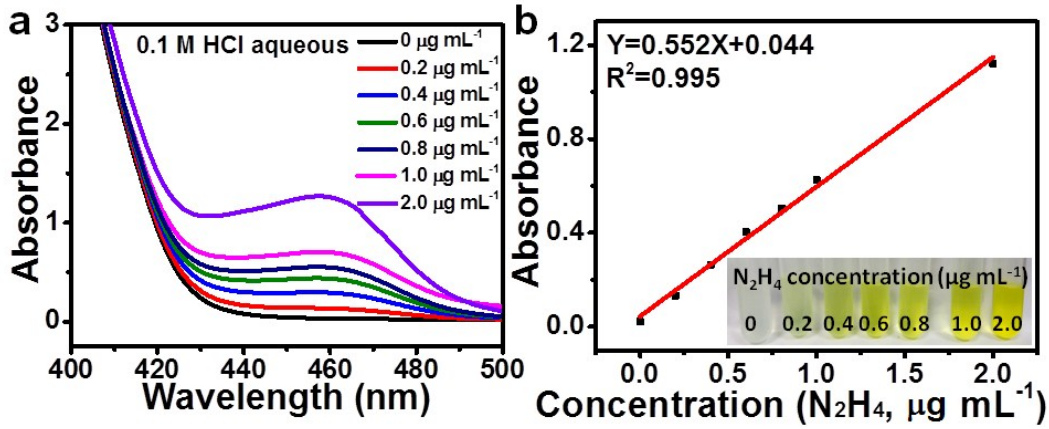

Fig. S4. (a) UV-Vis spectra of various N_2H_4 concentrations after incubated for 15 min at room temperature. (b) Calibration curve used for calculation of N_2H_4 concentrations.

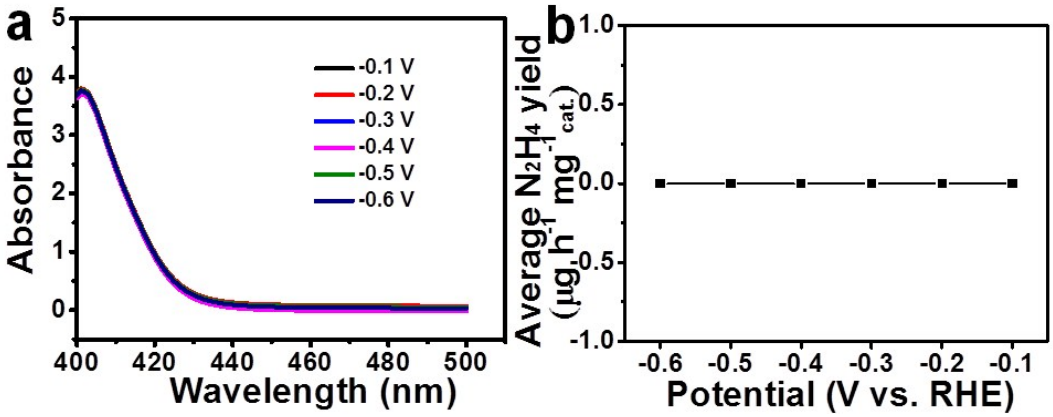

Fig. S5. (a) UV-Vis absorption spectra of the electrolytes estimated by the method of Watt and Chrisp after 2-h electrolysis at each given potential under ambient conditions. (b) N_2H_4 yields at each given potential.

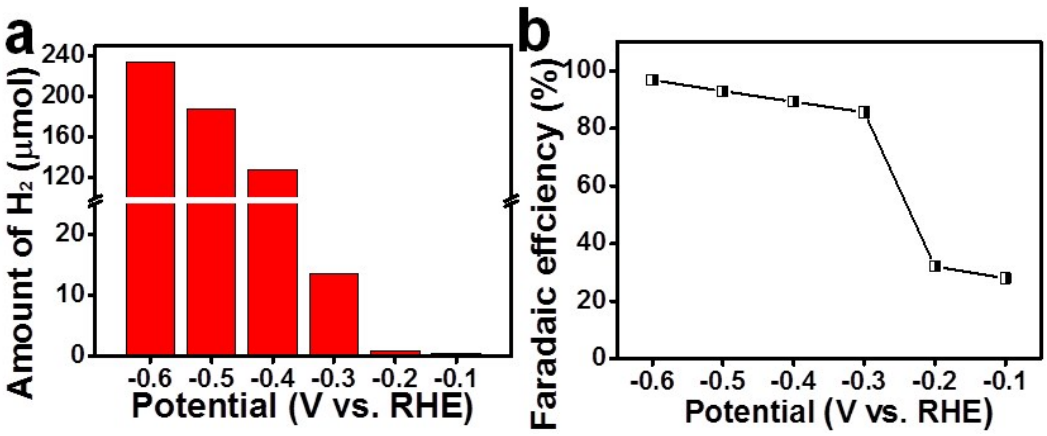

Fig. S6. (a) The amount of produced H_2 at each given potential. (b) The corresponding FE of HER at each given potential.

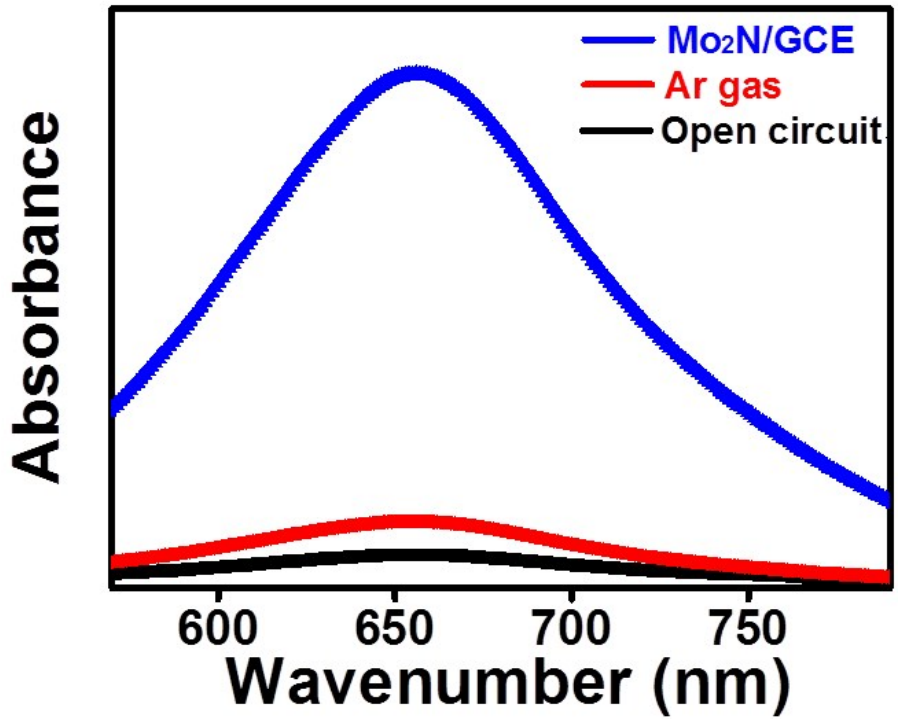

Fig. S7. UV-Vis absorption spectra of the electrolyte stained with indophenol indicator after charging at –0.3 V vs. RHE for 2 h under different electrochemical conditions.

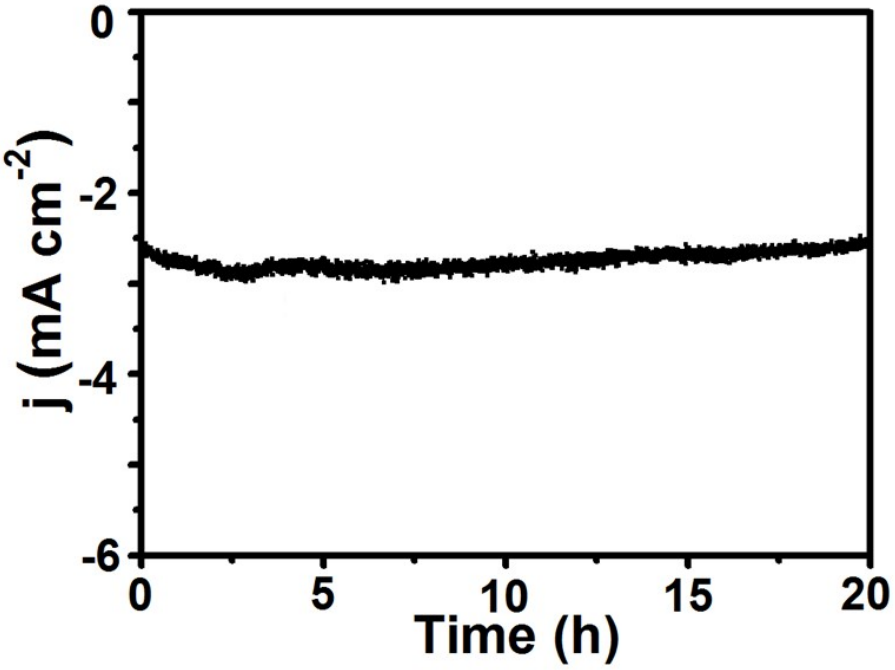

Fig. S8. Chrono-amperometry curve at potential of –0.3 V using Mo_2N/GCE for 20 h electrolysis.

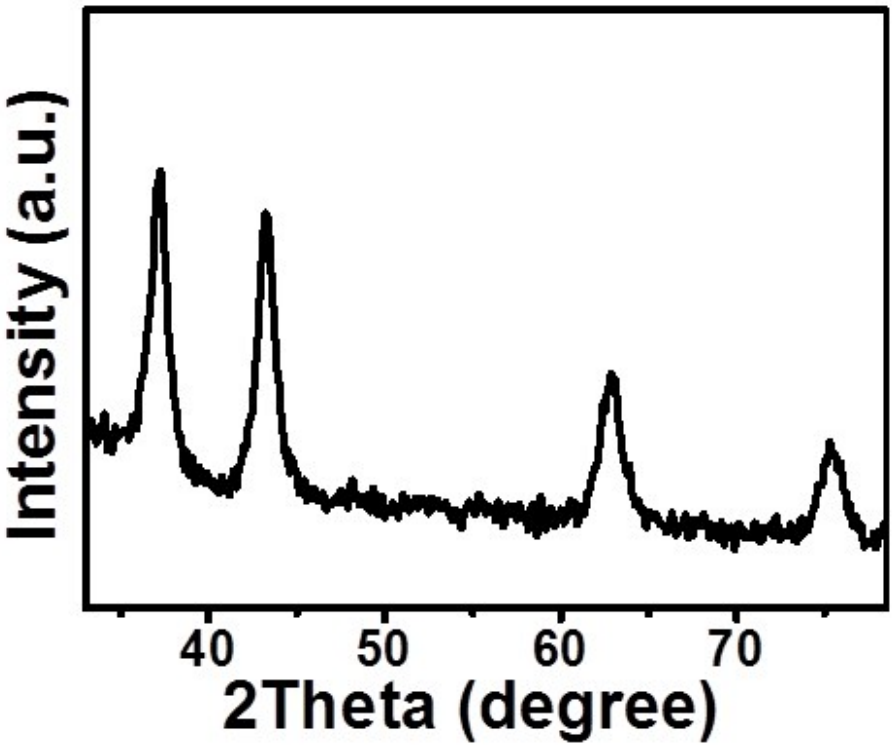

Fig. S9. XRD pattern for Mo_2N after stability test.

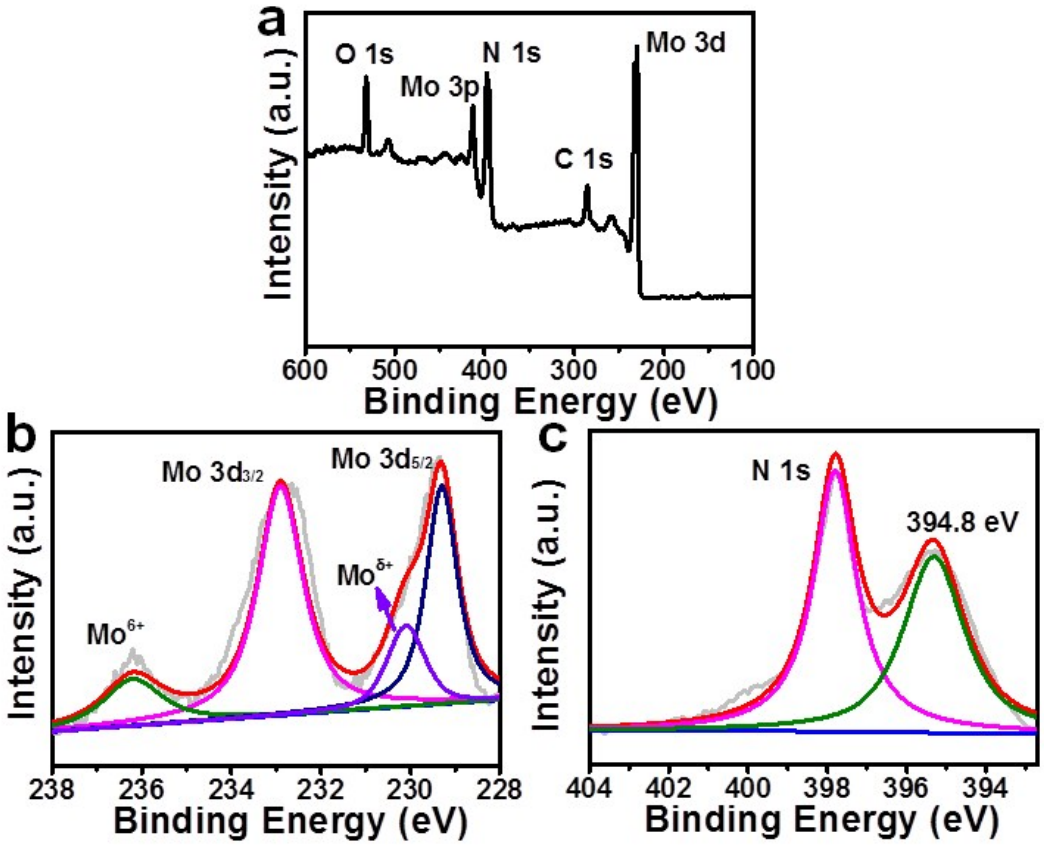

Fig. S10. (a) XPS survey spectrum of Mo_2N after 20 h electrolysis. XPS spectra in the (b) Mo 3d and (c) N 1s regions for Mo_2N after 20 h electrolysis.

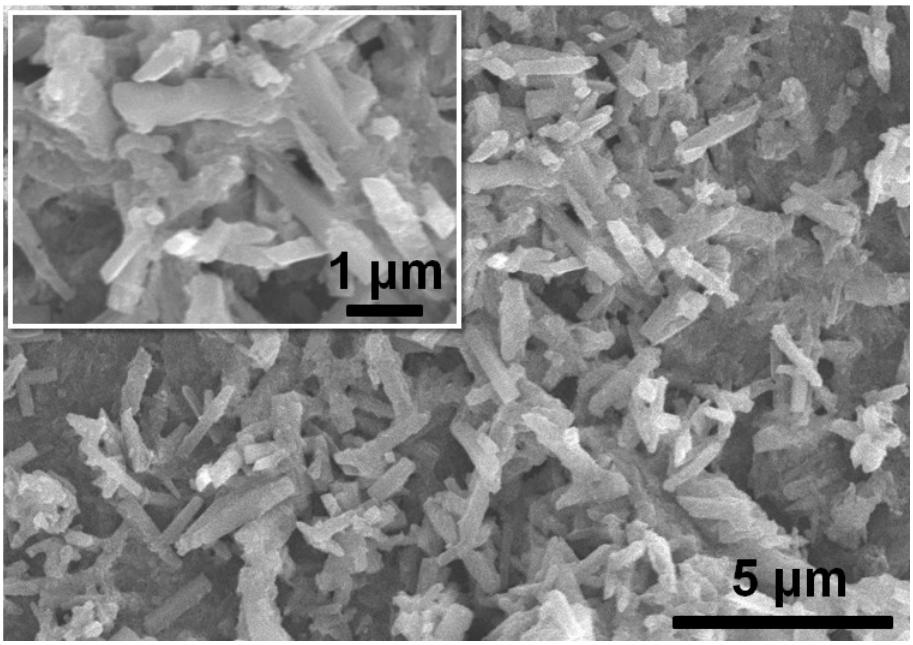

Fig. S11. SEM images for Mo_2N after stability test.

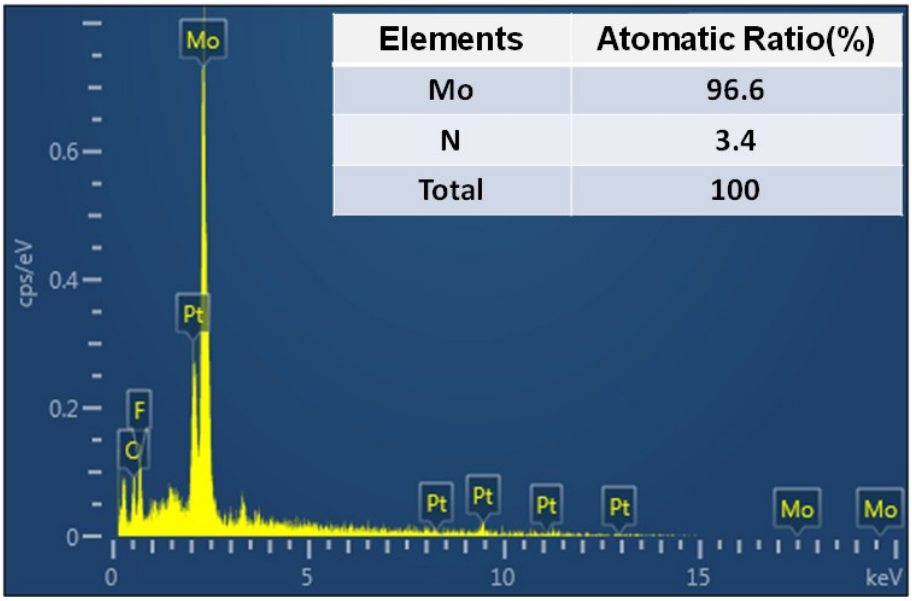

Fig. S12. EDX spectrum of Mo_2N after long term NRR in Ar-saturated HCl (the elements of C and F come from the conducting resin, the Pt element comes from the sprayed conducting layer).

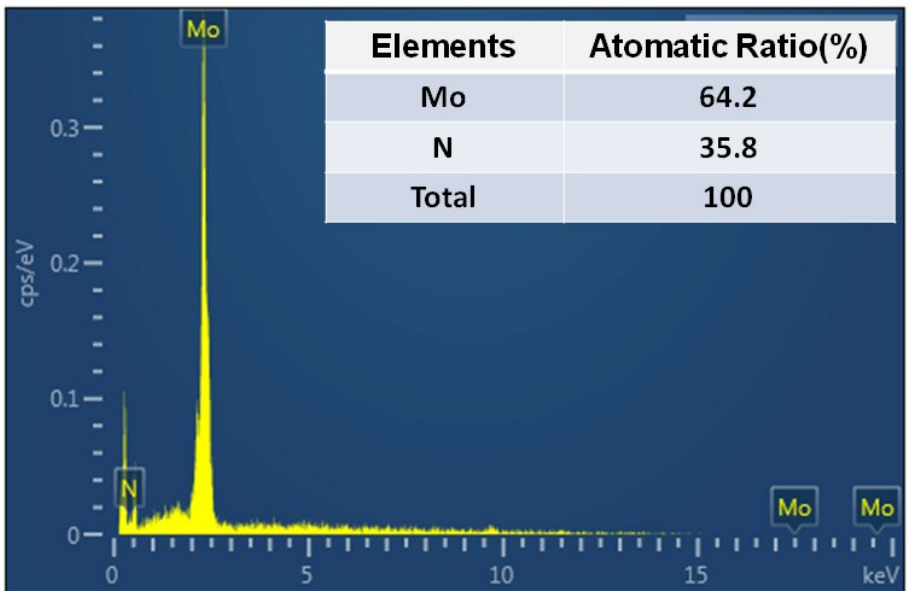

Fig. S13. EDX spectrum of Mo_2N after long term NRR in N_2-saturated HCl.

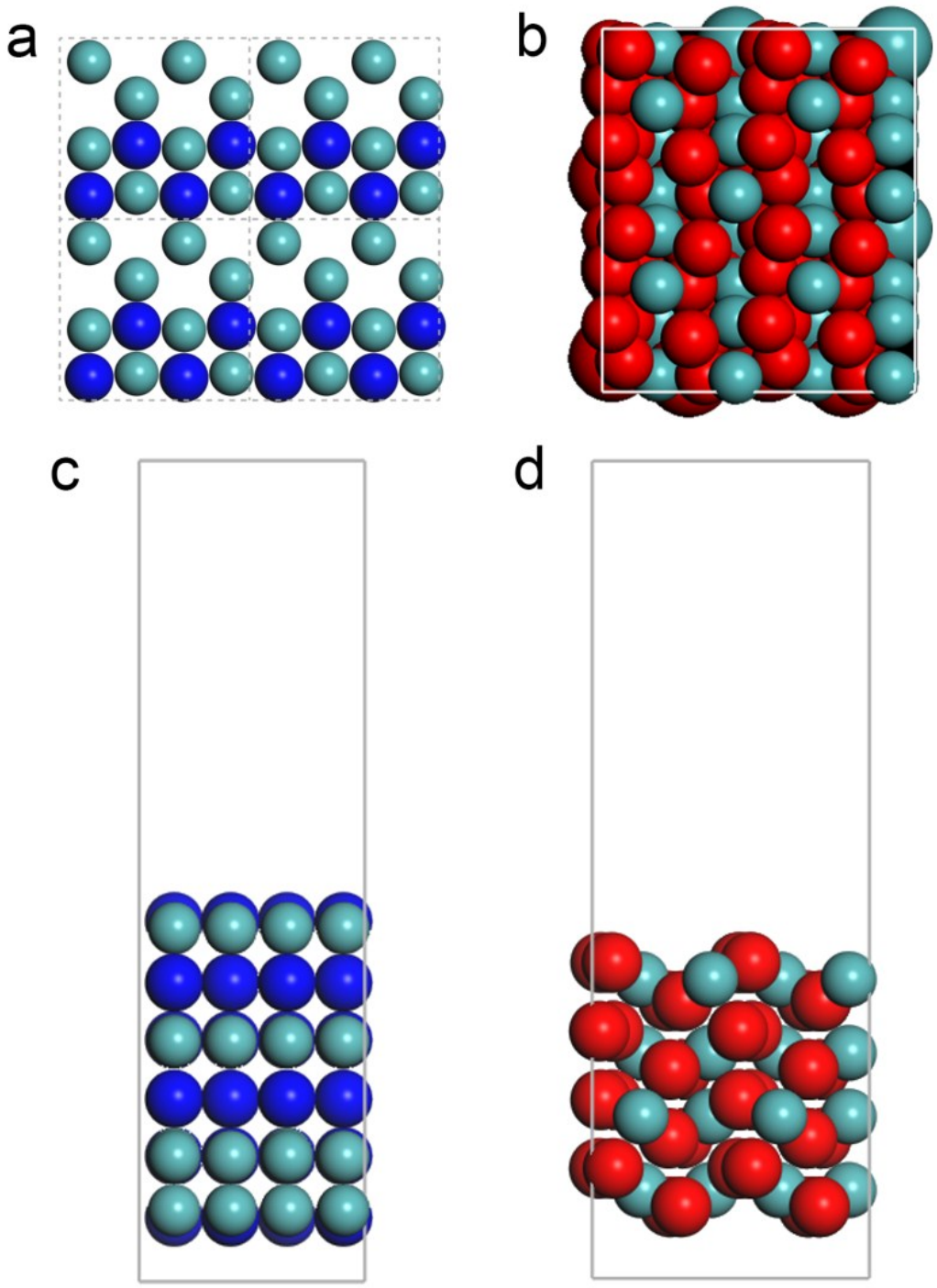

Fig. S14. (a) Top view of the first layer of 2×2×1 $Mo_2N(100)$ supercell. (b) Top view of $MoO_2(100)$ model. (c) Side view of $Mo_2N(100)$ slab model. (d) Side view of $MoO_2(100)$ slab model. Color code: Mo, cyan; N, blue; O, red.

Table S1. Comparison of the NH_3 electrosynthesis activity for Mo_2N/GCE with other NRR catalysts under ambient conditions.

Catalyst	r_{NH3}	FE%	Ref
Mo_2N/GCE	**78.4 μg h^{-1} mg^{-1}**	**4.5%**	**This work**
Mo nanofilm	3.09×10^{-11} mol s^{-1} cm^{-2}	0.72%	5
MoS_2/CC	8.08×10^{-11} mol s^{-1} cm^{-2}	1.17%	6
MoO_3 nanosheet	29.43 μg h^{-1} $mg^{-1}_{cat.}$	1.9%	7
$Bi_4V_2O_{11}/CeO_2$	23.21 μg h^{-1} $mg^{-1}_{cat.}$	10.16%	8
TA-reduced Au/TiO_2	21.4 μg h^{-1} $mg^{-1}_{cat.}$	8.11%	9
α-Au/CeO_x-RGO	8.31 μg h^{-1} $mg^{-1}_{cat.}$	10.1%	10
Au nanorod	6.042 μg h^{-1} $mg^{-1}_{cat.}$	~4.0%	11
γ-Fe_2O_3	0.212 μg h^{-1} $mg^{-1}_{cat.}$	1.9%	12
Fe_2O_3/CNTs	3.59×10^{-12} mol s^{-1} cm^{-2}	0.15%	13
N-doped nanocarbon	27.2 μg h^{-1} $mg^{-1}_{cat.}$	1.42%	14

Table S2. Comparison of the NH_3 electrosynthesis activity for Mo_2N/GCE with other catalysts under harsh conditions.

Catalyst	**Conditions**	**r_{NH3}**	**FE**	**Ref.**
Mo_2N/GCE	**25 °C**	**78.4 μg h^{-1} mg^{-1}**	**4.5%**	**This work**
Porous Ni	450 °C	1.54×10^{-11} mol s^{-1} cm^{-2}	0.9%	15
Ag	550 °C	2.94×10^{-14} mol s^{-1} cm^{-2}	0.46%	16
$La_{0.8}Cs_{0.2}Fe_{0.8}Ni_{0.2}O_{3-\delta}$	600 °C	1.23×10^{-10} mol s^{-1} cm^{-2}	0.55%	17

Table S3. The surface energies, E_{surf}, of various facets of Mo_2N and MoO_2. In the table below, E_{surf}s are in meV.

	Surface index				
	100	110	111	011	001
Mo_2N	108.5	158.2	165.5	168.3	108.5
MoO_2	72.7	102.6	116.3	91.8	127.2

References

1 G. Kresse and J. Furthmüller, *Phys. Rev. B*, 1996, **54**, 11169–11186.

2 J. P. Perdew, K. Burke and M. Ernzerhof, *Phys. Rev. Lett.*, 1996, **77**, 3865–3868.

3 P. E. Blochl, *Phys. Rev. B*, 1994, **50**, 17953–17979.

4 W. Atkins, Physical Chemistry, 6th ed.; Oxford University Press: Oxford, 1998, **485**, 866–867.

5 D. Yang, T. Chen and Z. Wang, *J. Mater. Chem. A*, 2017, **5**, 18967–18971.

6 L. Zhang, X. Ji, X. Ren, Y. Ma, X. Shi, Z. Tian, A. M. Asiri, L. Chen, B. Tang and X. Sun, *Adv. Mater.*, 2018, **30**, 1800191.

7 J. Han, X. Ji, X. Ren, G. Cui, L. Li, F. Xie, H. Wang, B. Li and X. Sun, *J. Mater. Chem. A*, 2018, DOI: 10.1039/C8TA03974G.

8 C. Lv, C. Yan, G. Chen, Y. Ding, J. Sun, Y. Zhou and G. Yu, *Angew. Chem.*, *Int. Ed.*, 2018, **57**, 6073−6076.

9 M. Shi, D. Bao, B. R. Wulan, Y. Li, Y. Zhang, J. Yan and Q. Jiang, *Adv. Mater.*, 2017, **29**, 1606550.

10 S. Li, D. Bao, M. Shi, B. Wulan, J. Yan and Q. Jiang, *Adv. Mater.*, 2017, **29**, 1700001.

11 D. Bao, Q. Zhang, F. Meng, H. Zhong, M. Shi, Y. Zhang, J. Yan, Q. Jiang and X. Zhang, *Adv. Mater.*, 2017, **29**, 1604799.

12 J. Kong, A. Lim, C. Yoon, J. H. Jang, H. C. Ham, J. Han, S. Nam, D. Kim, Y.-E. Sung, J. Choi and H. S. Park, *ACS Sustain. Chem. Eng.*, 2017, **5**, 10986–10995.

13 S. Chen, S. Perathoner, C. Ampelli, C. Mebrahtu, D. Su and G. Centi, *Angew. Chem.*, *Int. Ed.*, 2017, **56**, 2699–2703.

14 Y. Liu, Y. Su, X. Quan, X. Fan, S. Chen, H. Yu, H. Zhao, Y. Zhang and J. Zhao, *ACS Catal.*, 2018, **8**, 1186−1191.

15 R. Lan, A. K. A. Alkhazmi, I. A. Amar and S. Tao, *Appl. Catal.*, *B*, 2014, **152**, 212–217.

16 D. S. Yun, J. H. Joo, J. H. Yu, H. C. Yoon, J. Kim and C. Yoo, *J. Power Sources*, 2015, **284**, 245–251.

17 R. Lan, K. A. Alkhazmi, I. A. Amar and S. Tao, *Electrochim. Acta*, 2014, **123**, 582–587.